EXPERIMENTAL STUDY ON FEMTOSECOND LASER MICROMACHINING OF GROOVES IN STAINLESS STEEL

K. Kuršelis, T. Kudrius, D. Paipulas, O. Balachninaitė, and V. Sirutkaitis

Laser Research Centre, Vilnius University, Saulėtekio 10, LT-10223 Vilnius, Lithuania
E-mail: kestutis.kurselis@ff.vu.lt

Laser micromachining of grooves having rectangular profile in stainless steel with high repetition rate femtosecond pulses was investigated. Wide range of process parameters, such as peak fluence (0.15–133 J/cm^2), pulse repetition rate (10–223 kHz), cumulative exposure dose, and liquid-assisted method for improving both machining efficiency and resultant structure quality was considered in order to provide understanding of underlying physical capabilities and limitations. Thereby the presence of optimal regimes for obtaining respectively maximum pulse energy utilization and maximum machining performance is proved. Logarithmic law of ablation rate for 400 fs laser pulses centred at 1030 nm with repetition rate of 25 kHz is confirmed for this type of machining.

Keywords: femtosecond micromachining, laser ablation, liquid-assisted ablation, rectangular grooves

PACS: 81.16.Rf, 81.20.Wk, 61.80.Ba

1. Introduction

Precise metal machining down to the sub-micrometre scale, which is required for applications ranging from automotive industry [1] to consumer electronics [2], medicine [3], and production of microelectromechanical systems [4] is a nontrivial task even for the most advanced latest technology. Due to rigorous requirements for processing precision, performance, surface quality, structural intactness, and capital cost at the same time, micromilling, microelectric discharge machining, electrochemical milling with ultrashort voltage pulses, and laser micromachining are considered as leading methods [5]. The following can be attributed as advantages of the latter: non-contact, requiring no consumables, and highly flexible [6].

According to well established experimental [7] and theoretical [8] knowledge, pulsed lasers, especially producing ultrashort pulses, can minimize the heat affected zone (HAZ), thus increasing metal machining precision and quality with decreasing pulse duration below several picoseconds, which is mainly attributed to minimizing thermal penetration depth to the scale of optical penetration distance during the process of energy deposition. Although the lateral resolution of direct laser writing (DLW) method [2], which is considered in this paper, is mainly limited by a focal spot, the resulting height resolution can reach below 10 nm [9],

thus further leading to post-treatment-free structures, with high reproducibility and excellent surface parameters [10].

It has been presumed that due to the lack of powerful laser sources [11] the femtosecond technology is usable only for scientific or small scale applications, however since the introduction of chirped pulse amplification (CPA) technique [12] noticeable advancement has been achieved. With the introduction of such promising gain medium materials as Yb:YAG and Yb:KGW, as well as advancement in laser diode sources, current industrially feasible designs of femtosecond solid state lasers are approaching average power of 1000 W with excellent values of efficiency, repetition rate, and beam quality [13, 14]. Together with increased robustness and development of industrial know-how for the application of current scientific knowledge, the expansion of femtosecond machining might be predicted.

At this point the importance to provide an insight into the capabilities and suitability of femtosecond laser based 2.5D milling of widely used industrial material, which is also suitable for aforementioned applications, namely the steel, must be emphasized. Conventionally, similar experimental works, concerning femtosecond steel micromachining, were carried out employing either 1 kHz Ti:Sapphire laser systems [8, 11, 15, 16], or pico- and nanosecond systems

Table 1. Femtosecond laser micromachining system characteristics.

Characteristic	Value
Laser: type, name	DPSS Yb:KGW, PHAROS
Producer	Light Conversion LTD
Wavelength (nm)	1030
Max. average power (W)	3*
Repetition rate (kHz)	1–350
Max. pulse energy (mJ)	0.165*
Beam diameter, $1/e^2$ (mm)	3.6*
Pulse duration (FWHM) (fs)	400*
Beam quality factor, M2	1.2
Polarization	linear
Positioning stages: producer	Aerotech
XY stage, model	ALS130-150
Max. translation speed	300 mm/s
Z stage, model	ANT-4V
Controlling software, producer	SCA, ALTECHNA Co. Ltd.

*May differ from the producer specified;
measured/set for the experiment.

[17, 18], although possibilities and advantages for machining performance by the usage of multi-kilohertz femtosecond systems has been affirmed [19, 20].

Therefore the main goal of the work described in this paper was to examine currently commercially available advanced laser system of this type (diode pumped solid state (DPSS), specified in the following chapter) for machining structures, that will both extend focused spot by DLW technique and provide data regarding machining performance with increased repetition rates.

2. Experiment

The experiment was conducted using commercial femtosecond laser micromachining system with main characteristics specified in Table 1. Laser beam focusing on the samples was achieved by a $f = 25$ mm focal length plano-convex lens. Samples used for the experiment were non-polished plates of stainless steel with thickness of 3 mm. No shielding gases were used. Pulse duration was monitored via means of autocorrelation technique; energy value was obtained by measuring average power before the focusing lens with thermal power sensors OPHIR 30A/3A. A combination of half-wave plate and thin film polarizer was used for laser power adjustment. Polarization of the incident beam was kept parallel to the scanning vector during all experiments.

Experiment consisted of three main parts determining the influence of: (i) peak fluence and cumulative exposure dose, (ii) repetition rate, (iii) liquid presence

Table 2. Laser machining parameters.

Parameter	Value/range
Peak fluence (J/cm^2)	0.15–133
Positioning speed (mm/s)	2.5–100
Repetition rate[i], (kHz)	25
Repetition rate[ii], (kHz)	10–220
Repetition rate[iii], (kHz)	50

[i] Experiments with variable peak fluence.
[ii] Experiments with variable rep. rate.
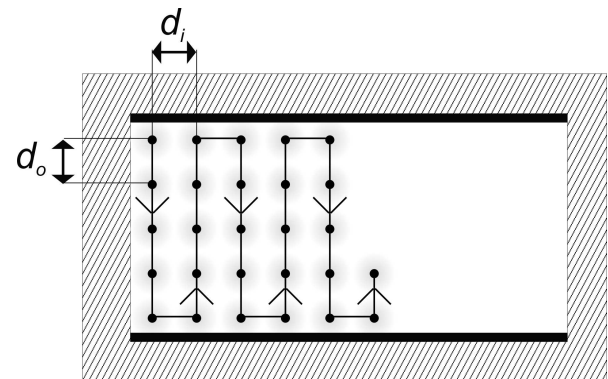[iii] Experiments with water-assisted ablation.

Fig. 1. Laser machining hatching scheme.

in the ablation zone. Detailed experimental parameters are given in Table 2.

All three experimental parts were carried out by machining rectangular grooves according to the scheme depicted in Fig. 1, where parameters d_o and d_i are respectively interpulse and interline (centre to centre) distance. In all cases pulse density in both directions was precisely controlled by setting translation speed and interline distance in such a manner that $d_o = d_i$, therefore implying cumulative exposure dose, which is extensively used through the text, expressed as

$$E_c = \frac{E_p}{d_o^2}, \tag{1}$$

where E_p denotes pulse energy.

In order to minimize geometry influence, all of the ablated grooves had a constant width of 50 μm. The first two experimental parts consisted of single-pass machining, third one being multi-pass machining, achieving predefined aspect ratio of 2:1. This part included examining such liquids as acetone (C_3H_6O, 99%), ethanol (C_2H_6O, 98%), and water (H_2O, distilled), chosen for having dispersed physical properties and being widely available.

The total count of 480 grooves was machined, that were later quantitatively analysed by optical confocal profiler Sensofar PLu 2300, whereas quality of grooves
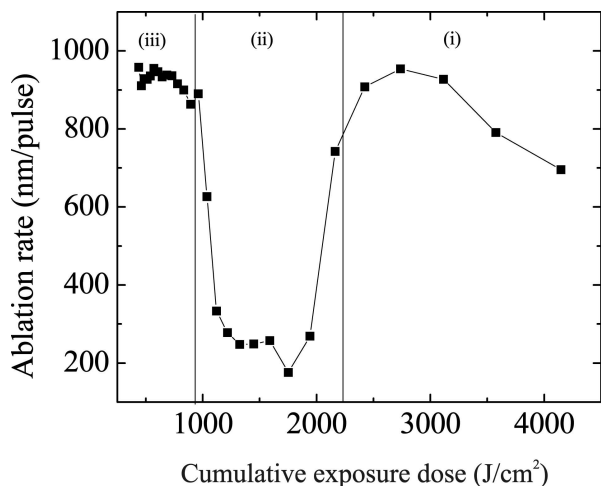
Fig. 2. Typical relationship between cumulative exposure dose and ablation rate at strong ablation regime ($\phi_0 = 133$ J/cm^2).

was examined by optical and SEM (Hitachi TM-1000) microscopes.

The choice of parameters for the first part was motivated by the requirement to cover wide range of peak fluence values (described as main factor influencing the performance [11]) under limited laser power. Repetition rate limitation of the second part was determined by limited available translation speeds (in order to keep pulse overlap constant) and pulse energy, the former two being defined by initial results, as explained in the discussion section.

The definition of peak laser fluence applied through this paper is, according to [21],

$$\phi_0 = \frac{2E_{\mathrm{p}}}{\pi w_0^2} \,, \qquad (2)$$

where w_0 is the Gaussian beam radius at $1/\mathrm{e}^2$ and the magnitude of former can be calculated from the following expression:

$$\omega_0 = \sqrt{\frac{d_c^2}{2\ln\left(\dfrac{\phi_0}{\phi_{\mathrm{th}}}\right)}} \,, \qquad (3)$$

with d_c being the diameter of the ablated crater and ϕ_{th} being the threshold peak ablation fluence.

3. Results and discussion

Two distinctive ablation regimes, determined by the value of peak fluence, namely strong and gentle ablation [22], exhibit diverse behaviour in respect of the cumulative exposure dose. Analysis of the machined samples revealed the existence of three different re-

gions in the case of strong ablation regime: (i) high cumulative exposure dose region with high removal rates (high depth at single pass), (ii) medium exposure region (poor performance, remelt, oxidation evident), (iii) low exposure region (best surface quality, high depth at single pass, fast scanning required). As an illustration for the observed dependencies see Fig. 2 which provides insight for machining at 133 J/cm^2 peak fluence. This can be attributed to higher energy diffusion and changing erosion front thus in turn changing absorption and ablation characteristics, with melting phase becoming more expressed. At high scanning rates the absorbing surface is close to the size of beam spot whereas slower rates result in translation of deep formation which provides the increase of absorbing surface and obstruction for plasma expansion from the deep structure, which helps to expel vapour and debris at the same time. The existence of region (ii) may be explained as an intermediate behaviour of former two. Since the scanning speed is reduced, the effective area at which energy is deposited allows more heat accumulation. At the same time, erosion front and structure depth still have not changed enough to enhance the material removal. It can be concluded here as well that increasing peak fluence requires higher scanning rates, e. g., minimal speed of 32.5 mm/s to reach regime (i) at 133 J/cm^2 and to observe material removal from the sample. Scanning at lower speed will result in emboss profile (Fig. 3).

The analysis of ablation rate, which has been estimated from profiling measurements as total removed volume divided by focal spot area and number of pulses, has been performed. The general picture of the ablation rates for various parameters can be analysed in Fig. 4, where ablation rates are plotted against cumulative exposure dose (proportional to scanning rate / pulse density) and peak pulse fluence on logarithmic-linear scale, which might be as a reference for choosing highest machining speed.

As can be seen in Fig. 5 this study provides quantitative data on femtosecond laser micromachining energy efficiency dependent on peak fluence and cumulative exposure dose. This information is of great importance when a laser machining process is being designed and requirements for the laser system are desired to be minimized. It is evident from the plot that this type of laser machining has the maximum around the boundary of gentle and strong ablation regimes, which corresponds to experimental peak fluence values ranging from 6.4 to 16.3 J/cm^2. In comparison with similar picosecond machining [17, 23], higher efficiency values are
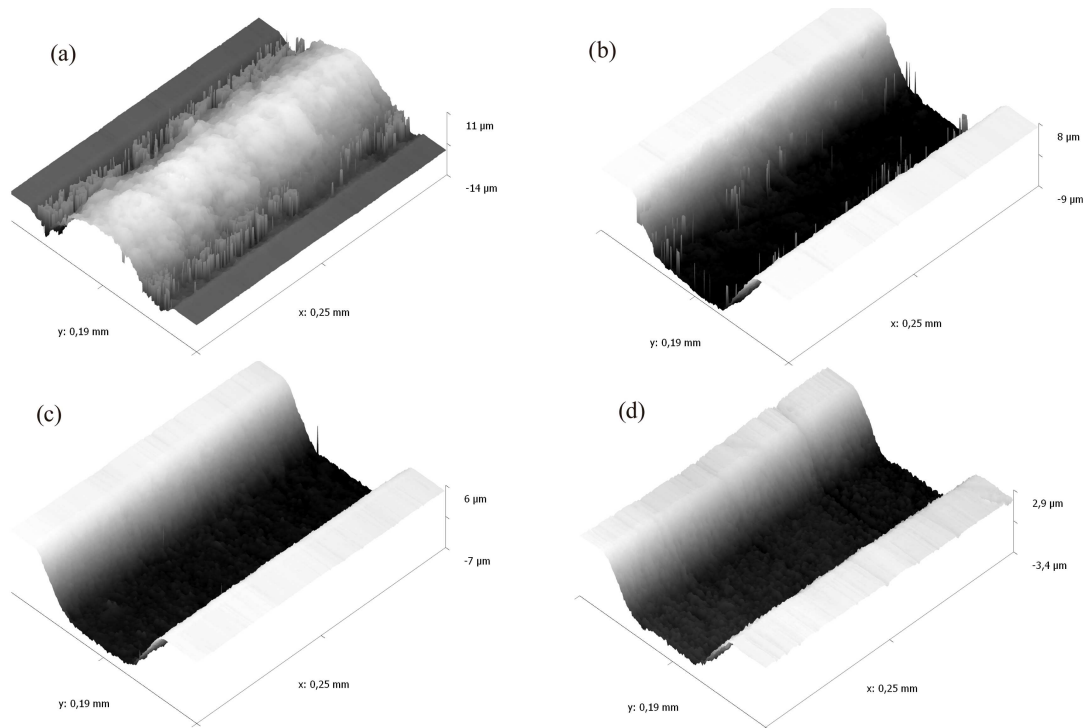
Fig. 3. Different ablation regimes, depending on cumulative exposure dose (scanning speed): (a) emboss profile, (b) regime (i), (c) regime (ii), (d) regime (iii).
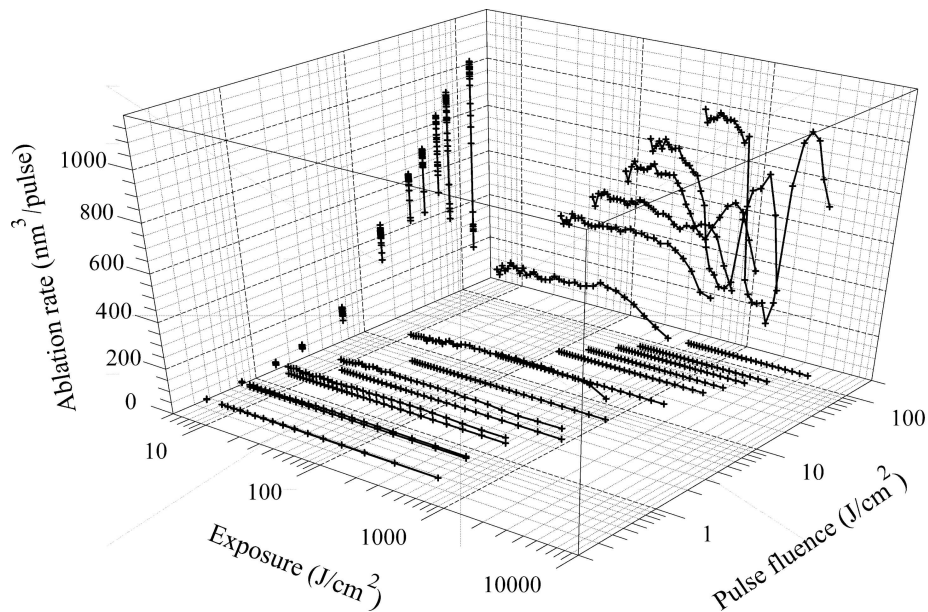

Fig. 4. Dependence of ablation rate on peak pulse fluence and cumulative exposure dose.

obtained, although at higher peak fluence. This in turn means that there is a possibility to have high machining resolution and at the same time retain performance.

As it can be seen in Fig. 4, material removal rate is highly sensitive to both variable parameters. Scanning speed window, which can be defined as values from those corresponding to emboss profile elimination up to creation of separate craters on the machined sur-face, gets shifted towards faster scanning as peak fluence increases, in result of both higher ablation depth and larger crater. This makes overall analysis complicated. However one can assume that data points in Fig. 4, which correspond to highest efficiency for each value of peak fluence in Fig. 5, may signify similar ablation conditions. This may also be observed in the projection of corresponding ablation rates on the plane
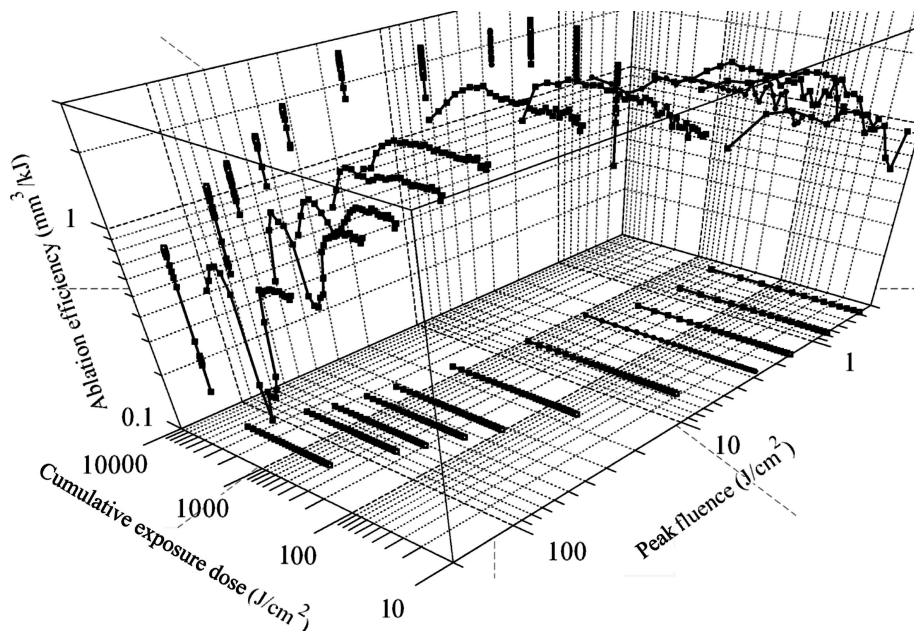
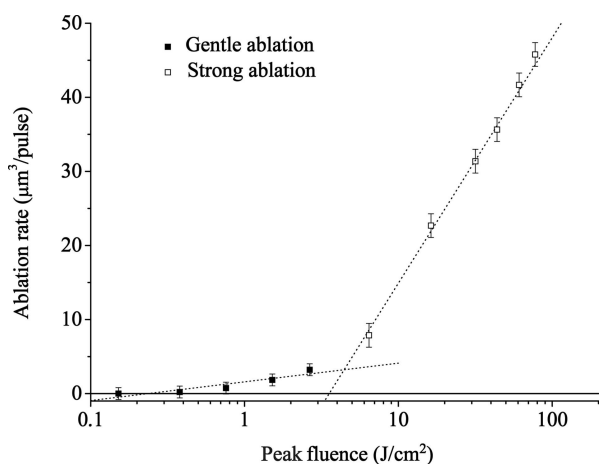Fig. 5. Material removal efficiencies as a function of cumulative exposure dose and peak laser fluence.

Fig. 6. Distinction of two ablation regimes.

Table 3. Characteristic values of different ablation regimes for 2.5D machining.

α^{-1} (nm)	γ (nm)	ϕ_{th}^{α} (J/cm^2)	ϕ_{th}^{γ} (J/cm^2)
10.31	21.33	0.24	3.55

regime, electron heat diffusion length, and strong ablation threshold, reveal values presented in Table 3.

It must be noted here that optical penetration and heat diffusion lengths obtained here are lower as well as ablation thresholds higher in comparison to literature [25], however longer pulse duration and longer centre wavelength must be taken into account [7]. It is also unclear what is the influence of higher repetition rate of pulses on the chemical surface processes, change of thermoreflectance and thermoabsorbance.

At a first glance one of the most straightforward ways to increase laser machining performance is to raise pulse repetition rate. At the same time out of practical considerations a high ablation efficiency is desired in order to utilize the lasing power to higher degree. In turn this might arise either from better energy deposition or from more efficient material removal, the latter providing advantages for precision due to minimized energy losses for undesired phenomena. Therefore, for the experiment with different repetition rates, two values of peak fluence and cumulative exposure dose that closely correspond to the highest previously obtained efficiency were chosen. It was observed that in the range of 10 to 223 kHz heat accumulation effects for these peak fluence values could be observed. Qualitatively it emerges as the formation of remelted material

perpendicular to ablation rate axis (Fig. 4). One can see two distinct regions which can be approximated with different logarithmic functions. These dependences in two dimensions are depicted in Fig. 6. Following [24], logarithmic fits of the form

$$L = \alpha^{-1} \ln\left(\frac{\phi_0}{\phi_{th}^{\alpha}}\right) \qquad (4)$$

and

$$L \approx \gamma \ln\left(\frac{\phi_0}{\phi_{th}^{\gamma}}\right), \qquad (5)$$

where L, α^{-1}, ϕ_0, ϕ_{th}^{α}, γ, ϕ_{th}^{γ} accordingly is ablation depth per single pulse, optical penetration depth, peak fluence, ablation threshold for gentle ablation

which experiences viscous flow, obstructing the machining process and degrading structure quality. This leads to degradation of nearby surface and sidewalls of the structure. As an example, for peak fluence value of $8.2 \, \mathrm{J/cm^2}$ this also results in decreased ablation rate, whereas for $16.3 \, \mathrm{J/cm^2}$ no groove could be formed at repetition rates exceeding 30 kHz (Fig. 7). It might be concluded here that in order to optimize laser machining parameters it is required to take into account not only peak laser fluence at the sample and single pass cumulative exposure dose, but also the machining power and material dependent heat dissipation. In other words, femtosecond laser micromaching has a great potential for material removal rate increase, however for the required resolution and surface quality there exists an upper boundary for maximizing it, which can be reached by careful adjustment of positioning speed with a given repetition rate and peak fluence.

It is important to note here that by adopting model proposed in [20] it is possible to evaluate the number of pulses required for melting in focal spot to occur by the following expression:

$$N_{\mathrm{melt}} = \frac{4\pi^{3/2} \, \kappa \, \sqrt{D} \, T_{\mathrm{melt}}}{\tau_{\mathrm{l}} \, A \, E_{\mathrm{p}}} \, \nu^{-5/2} , \qquad (6)$$

where κ is the thermal conductivity of the material, D is thermal diffusivity, T_{melt} is melting temperature, A is absorptivity, ν is laser repetition rate, τ_{l} is pulse duration, and E_{p} is pulse energy. In the case of steel, even for highest repetition rates applied for groove machining experiments being discussed in this paper, the local heat accumulation is considered negligible. However this model does not take into account residual sample heating, described in [26], and neglects effects present particularly in 2D machining. As such the change of erosion front and modification of absorbing material together with damage accumulation [25] must be noted. The latter can be explained by high porosity of debris, deposited in the vicinity of the focal spot, which at the same time leads to decreased heat diffusion and conduction together with better absorption properties, which can further lead to accumulation effects at lower repetition rates.

Since the single-pass machining resulted in a maximal groove depth of approx. 20 μm, multipass machining was examined. Quality degradation and groove narrowing at higher aspect ratios, which has been observed for various materials in single-line experiments by other authors [27, 28], was evident for wide groove machining as well. These effects have increased with higher repetition rates and peak fluence values. As a
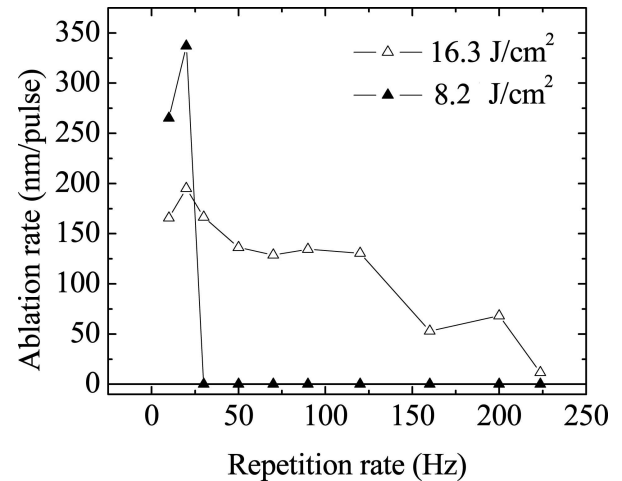
Fig. 7. Ablation rate as a function of laser repetition rate.

typical example, examination of the sidewalls for peak fluence of $8.2 \, \mathrm{J/cm^2}$, repetition rate of 50 kHz, 10 passes also revealed irregular surface morphology with roughness as high as $R_a = 12 \, \mu$m, partial porous debris filling, and variable groove depth.

There has been done various experimental research with liquid assistance for laser machining [29–31]. This has motivated laser steam cleaning for the machining of rectangular grooves in steel to be examined. High aspect ratio grooves are difficult to machine mostly due to obstruction for plasma plume expansion and accordingly material removal, which then tends to stick to sidewalls. It is proposed that depending on laser parameters irradiated liquids can experience formation of the shock wave, vapour expansion, cavitations, and breakdown [30, 32]. All these phenomena primarily result in disturbance of incident beam, increased laser power losses, and irregularities of machining, although values for surface roughness and cleanliness can be enhanced. Thereinafter the method of capillary wetting was examined. This method relies on self propagation of liquid along narrow channel due to surface tension, thus resulting in high homogeneity and minimal liquid film thickness. It was experienced that mainly due to different surface tension and volatility values the results were contrasting: high value of water surface tension led to convexity and degradation of machining precision due to beam refraction; acetone wetting resulted in a minimal influence, due to high volatility further increased by bulk heating of the sample; ethanol proved to be the most suitable for this purpose. For every liquid in consideration the application onto groove was repeated after single pass machining resulting in periodical cleaning of the groove, thus minimizing negative impact of fluid. Experimental results show that
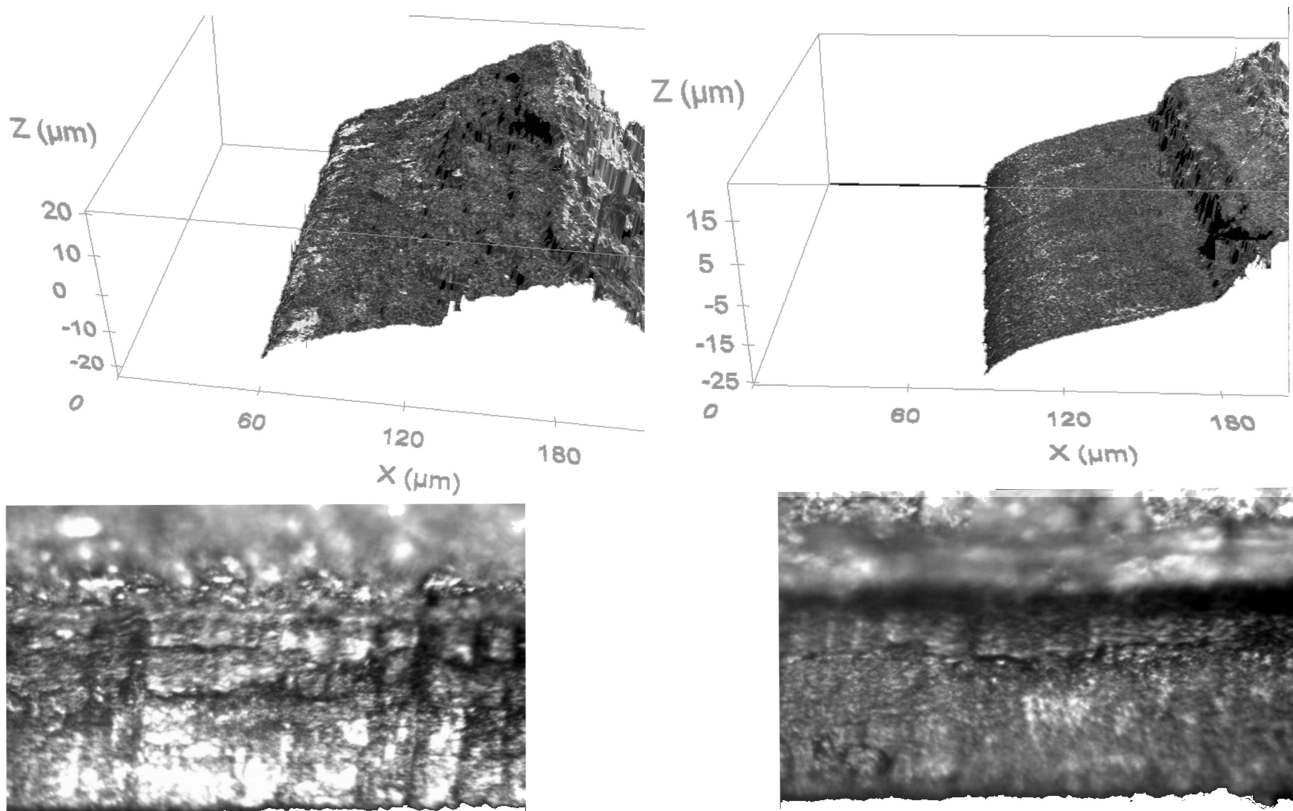
Fig. 8. Effect of ethanol assistance for narrow groove machining. Left: conventional multipass machining; right: with capillary applied ethanol.

by this method it is possible to improve surface quality of the sidewalls, increase maximal depth and performance of machining of high aspect ratio grooves, which have widths close to the characteristic plasma plume size [16]. Some side effects to mention is reduced sticking of the particles to the sample surface, nanoparticle dust pollution, and machining noise, however the method involves additional technological challenge to supply required amount of liquid to processing place in a precise manner. Figure 8 depicts difference in ethanol assisted ablation compared to conventional ablation results.

4. Conclusions

Direct laser machining of grooves in steel is a complex task, which requires to take into account these main influencing factors: (i) erosion front change due to ongoing ablation, (ii) material removal obstruction in higher depths, (iii) increment of thermal effects with increasing repetition rate. Energy deposition rate and consequently maximal machining speed has an upper limit, which is mainly determined by the peak pulse fluence at sample surface, repetition rate, and material properties. Concluding from experimental results it is possible to determine optimal peak fluence at the processed surface together with scanning rate and interline shift for fabrication of rectangular profile grooves in order to maximize either material removal rate or energetic efficiency. Experiments of steel ablation for fabrication of deep rectangular profile grooves in the presence of liquids reveal that properly chosen type of fluid and its dosage can improve (i) wall quality, (ii) machining performance, (iii) conditions of working environment.

Acknowledgements

References

[1] M.R.H. Knowles, A.I. Bell, G.R. Rutterford, A.J. Andrews, G. Foster-Turner, and A.J. Kearsley, Laser drilling of fuel injection components, in: *Proceedings of ICALEO 2000*, Vol. 91 (Society of Photo-Optical

Instrumentation Engineers, Bellingham, USA, 2000) pp. F42–F51.

[2] K. Sugioka, B. Gu, and A. Holmes, The state of the art and future prospects for laser direct-write for industrial and commercial applications, MRS Bull. **32**, 47–54 (2007).

[3] C. Momma, U. Knop, and S. Nolte, Laser cutting of slotted tube coronary stents – State-of-the-art and future developments, Progr. Biomed. Res. **4**, 39–44 (1999).

[4] A.S. Holmes, Laser fabrication and assembly processes for MEMS, Proc. SPIE **4274**, 297–306 (2001).

[5] L. Uriarte, A. Ivanov, H. Oosterling, L. Staemmler, P.T. Tang, and D. Allen, A comparison between microfabrication technologies for metal tooling, in: *4M 2005, First International Conference on Multi-Material Manufacture Proceedings*, eds. W. Menz and S. Dimov (Elsevier Science, Oxford, UK, 2005) pp. 351–354.

[6] M. Henry, P.M. Harrison, I. Henderson, and M.F. Brownell, Laser milling: a practical industrial solution for machining a wide variety of materials, Proc. SPIE **5662**, 627–632 (2004).

[7] C.Y. Chien and M.C. Gupta, Pulse width effect in ultrafast laser processing of materials, Appl. Phys. A **81**, 1257–1263 (2005).

[8] B.N. Chichkov, C. Momma, S. Nolte, F. von Alvensleben, and A. Tünnermann, Femtosecond, picosecond and nanosecond laser ablation of solids, Appl. Phys. A **63**, 109–115 (1996).

[9] S.E. Kirkwood, M.T. Taschuk, Y.Y. Tsui, and R. Fedosejevs, Nanomilling surfaces using near-threshold femtosecond laser pulses, J. Phys. Conf. **59**(1), 591–594 (2007).

[10] G. Kamlage, T. Bauer, A. Ostendorf, and B.N. Chichkov, Deep drilling of metals by femtosecond laser pulses, Appl. Phys. A **77**, 307–310 (2003).

[11] R. Le Harzic, D. Breitling, M. Weikert, S. Sommer, C. Fohl, S. Valette, C. Donnet, E. Audouard, and F. Dausinger, Pulse width and energy influence on laser micromachining of metals in a range of 100 fs to 5 ps, Appl. Surf. Sci. **249**, 322–331 (2005).

[12] D. Strickland and G. Mourou, Compression of amplified chirped optical pulses, Opt. Commun. **56**, 219–221 (1985).

[13] T. Eidam, S. Hanf, E. Seise, T. V. Andersen, T. Gabler, C. Wirth, T. Schreiber, J. Limpert, and A. Tünnermann, Femtosecond fiber CPA system emitting 830 W average output power, Opt. Lett. **35**, 94–96 (2010).

[14] P. Russbueldt, T. Mans, G. Rotarius, J. Weitenberg, H.D. Hoffmann, and R. Poprawe, 400W Yb:YAG Innoslab fs-Amplifier, Opt. Express **17**, 12230–12245 (2009).

[15] F. Dausinger, Femtosecond technology for precision manufacturing: fundamental and technical aspects, Proc. SPIE **4830**, 471–478 (2003).

[16] J. König, S. Nolte, and A. Tünnermann, Plasma evolution during metal ablation with ultrashort laser pulses, Opt. Express **13**, 10597–10607 (2005).

[17] R. Penttilä, H. Pantsar, and P. Laakso, Picosecond laser processing – material removal rates of metals, in: *Proceedings of the 11th NOLAMP Conference in Laser Processing of Materials* (Lappeenranta University of Technology, Lappeenranta, Finland, 2007) pp. 502–512.

[18] D.M. Karnakis, G. Rutterford, and M.R.H. Knowles, High power DPSS laser micro-machining of silicon and stainless steel, in: *Proceedings of the 3rd International WLT Conference on Lasers in Manufacturing* (AT-Fachverlag, Stuttgart, Germany, 2005) pp. 741–746.

[19] A. Ostendorf, C. Kulik, T. Bauer, and N. Barsch, Ablation of metals and semiconductors with ultrashort-pulsed lasers, improving surface qualities of micro cuts and grooves, Proc. SPIE **5340**, 153–163 (2004).

[20] A. Ancona, F. Röser, K. Rademaker, J. Limpert, S. Nolte, and A. Tünnermann, High speed laser drilling of metals using a high repetition rate, high average power ultrafast fiber CPA system, Opt. Express **16**, 8958–8968 (2008).

[21] J.M. Liu, Simple technique for measurements of pulsed Gaussian-beam spot sizes, Opt. Lett. **7**, 196–198 (1982).

[22] R. Stoian, D. Ashkenasi, A. Rosenfeld, and E.E.B. Campbell, Coulomb explosion in ultra-short pulsed laser ablation of Al_2O_3, Phys. Rev. B **62**, 13167–13173 (2000).

[23] G. Račiukaitis, M. Brikas, P. Gečys, B. Voisiat, and M. Gedvilas, Use of high repetition rate and high power lasers in microfabrication: How to keep the efficiency high?, J. Laser Micro/Nanoeng. **4**(3), 186–191 (2009).

[24] S. Preuss, A. Demchuk, and M. Stuke, Sub-picosecond UV laser ablation of metals, Appl. Phys. A **61**, 33–37 (1995).

[25] P.T. Mannion, J. Magee, E. Coyne, G.M. O'Connor, and T.J. Glynn, The effect of damage accumulation behaviour on ablation thresholds and damage morphology in ultrafast laser micro-machining of common metals in air, Appl. Surf. Sci. **233**, 275–287 (2004).

[26] A.Y. Vorobyev, V.M. Kuzmichev, N.G. Kokody, P. Kohns, J. Dai, and Ch. Guo, Residual thermal effects in Al following single ns- and fs-laser pulse ablation, Appl. Phys. A **82**(2), 357–362 (2006).

[27] A. Borowiec and H.K. Haugen, Femtosecond laser micromachining of grooves in indium phosphide, Appl. Phys. A **79**, 521–529 (2004).

[28] F. Ahmed and M.S. Lee, Micromachining of grooves for cutting fused silica plates with femtosecond laser

pulses, in: *Conference on Lasers and Electro-Optics / Pacific Rim 2007* (Optical Society of America, 2007), paper TuB2_3.

[29] M. Geiger, S. Roth, and W. Becker, Microstructuring and surface modification by excimer laser machining under thin liquid films, Proc. SPIE **3404**, 200–208 (1998).

[30] A. Dupont, P. Caminat, and P. Bournot, Enhancement of material ablation using 248, 308, 532, 1064 nm laser pulse with a water film on the treated surface, J. Appl.

Phys. **78**, 2022–2028 (1995).

[31] A.C. Tam, P.L. Wing, W. Zapka, and W. Ziemlich, Laser-cleaning techniques for removal of surface particulates, J. Appl. Phys. **71**(7), 3515–3523 (1992).

[32] R. Brinkmann, C. Hansen, D. Mohrenstecher, M. Scheu, and R. Birngruber, Analysis of cavitation dynamics during pulsed laser tissue ablation by optical on-line monitoring, IEEE J. Select. Topics Quantum Electron. **2**, 826–835 (1996).

EKSPERIMENTINIS ITIN MAŽŲ GRIOVELIŲ FORMAVIMO NERŪDIJANČIAME PLIENE FEMTOSEKUNDINIU LAZERIU TYRIMAS

K. Kuršelis, T. Kudrius, D. Paipulas, O. Balachninaitė, V. Sirutkaitis

Vilniaus universitetas, Vilnius, Lietuva

Santrauka

Tirtas stačiakampio profilio griovelių, kurių charakteringi matmenys yra didesni nei sufokusuoto pluošto diametras, formavimo, naudojant didelio pasikartojimo dažnio femtosekundinius impulsus, dėsningumai. Šiuo tikslu plačiame diapazone buvo keičiamos pagrindinių tokiam apdirbimui svarbių parametrų vertės: impulsų pasikartojimo dažnis (10–223 kHz), impulso energijos įtėkis (0,15–133 J/cm^2), spinduliuotės dozė. Išbandytas suaktyvinimo skysčiu metodas, leidžiantis pagerinti tiek apdirbimo proceso, tiek ir gau-

namo darinio charakteristikas. Gauti rezultatai padeda lengviau įvertinti šios technologijos galimybes ir suprasti vykstančius fizikinius procesus. Iš jų matyti, kad, tinkamai parinkus parametrus, galima maksimaliai panaudoti spinduliuotės energiją ir pasiekti didžiausią našumą. Taip pat buvo parodyta, kad, naudojant 400 fs 1030 nm centrinio bangos ilgio impulsus ir esant 25 kHz pasikartojimo dažniui, šiam apdirbimo būdui galioja logaritminis abliacijos spartos priklausomybės nuo energijos įtėkio dėsnis.